The Linnean Society of London
BIOLOGICAL Journal of the Linnean Society

Historical diversification and biogeography of the endemic southern African dung beetle genus, Epirinus (Scarabaeidae: Scarabaeinae)

Journal:	*Biological Journal of the Linnean Society*
Manuscript ID	BJLS-6558.R2
Manuscript Type:	Original article
Date Submitted by the Author:	11-Mar-2021
Complete List of Authors:	Daniel, Gimo; National Museum, Bloemfontein, Terrestrial Invertebrates Sole, Catherine; University of Pretoria, Zoology and Entomology; Scholtz, CH Davis, Adrian
Keywords:	climatic changes, geological uplift, molecular phylogeny, ecological niche modelling

Historical diversification and biogeography of the endemic southern African dung beetle genus, *Epirinus* (Scarabaeidae: Scarabaeinae)

GIMO M. DANIEL[1,2*], CATHERINE L. SOLE[1], CLARKE H. SCHOLTZ[1] & ADRIAN L.V. DAVIS[1]

[1]Department of Zoology & Entomology, University of Pretoria, Private Bag X20, Hatfield, 0028 South Africa.

[2]Department of Terrestrial Invertebrates, The National Museum, 36 Aliwal Street, Bloemfontein, South Africa.

[*]Corresponding author. E-mail: gimo.daniel@nasmus.co.za.

Running title: Evolution and speciation of *Epirinus*

ABSTRACT

The role of the geological uplift and climatic changes during the late Cenozoic on the species diversification of southern African dung beetles is not fully understood. Therefore, we use a divergence-time-estimated phylogeny, macroevolutionary analyses and ecological niche modelling under different climatic scenarios to investigate diversification of the endemic southern African genus, *Epirinus*. We predict the ancestral range and vegetation type occupied by *Epirinus* and how late Cenozoic climatic fluctuations and resulting vegetation changes affected speciation and extinction of *Epirinus* species. Our results suggest that the genus originated in forest with radiation into three geographical centres: (a) northeast escarpment forest and highland grassland; (b) southeast forest and (c) southwest lowlands to northeast uplands in open vegetation. Reduced speciation rates in the mid-Miocene and increased extinction rates during the drier and cooler Plio-Pleistocene coincide with the replacement of forest by grassland or savanna in southern Africa. Drier climate in southern Africa may have driven extensive contraction of shaded vegetation, forcing an adaptation of forest inhabitants to upland grassland environments, or driving *Epirinus* species to extinction. Our study supports hypotheses of climatically driven diversification of *Epirinus* whereas ecological niche modelling across different geological periods suggest that the southeast and, to a lesser extent, the west coast of South Africa as stable areas.

Keywords: climatic changes, geological uplift, molecular phylogeny, ecological niche modelling.

INTRODUCTION

Understanding mechanisms and processes that have driven current spatial distribution in biodiversity is one of the main objectives of historical biogeography. The world-wide evolutionary history of the dung beetle subfamily, Scarabaeinae (Coleoptera: Scarabaeidae), has been associated with their key ecological specialization to vertebrate / mammal dung, which is exploited for both feeding and breeding (Halffter & Matthews, 1966; Davis & Scholtz, 2001). It is also hypothesised that regional taxon diversification and distribution patterns of dung beetles have been

driven by the interaction between two principal physical factors, the effects of global climatic shifts and geomorphological changes (Davis & Scholtz, 2010). In southern Africa, endemism of many dung beetle species is presumably attributed to geological events and climatic changes during the Mio-Pliocene epoch (Davis, 1997; Sole, Scholtz, & Bastos, 2005; Daniel *et al.*, 2020a; Davis & Scholtz, 2020). However, specific research questions on whether these late Cenozoic trends have driven high endemism of dung beetles in the region are not fully addressed.

Geological references concur that there was late Cenozoic uplift in southeast Africa that created the central southern African plateau, including, the Drakensberg, Highveld and Upper Karoo (King, 1944; Partridge & Maud, 1987; Paul, Roberts, & White, 2014; Dauteuil, Bessin, & Guillocheau, 2015; Rudge *et al.*, 2015). These orogenic events led to a drop in temperature over the upland regions (Haddon & McCarthy, 2005; Dauteuil *et al.*, 2015). Coevally with uplift, the southwest of southern Africa underwent a climatic change from an earlier subtropical summer rainfall system (Sciscio *et al.*, 2016) to cooler winter rainfall or late summer arid climatic systems. The inception of the winter rainfall system in the Pliocene (Deacon, 1983) resulted from the expansion of westerly wind currents from the south Atlantic Ocean following permanent south polar glaciation during the mid-late Miocene (Deacon, 1983). The southwest arid region is associated with upwelling of the cold Benguela current on the west coast. The summer rainfall climate to the northeast is associated with expansion of easterly wind currents centred over the Indian Ocean (Tyson, 1986; Chase & Meadows, 2007; Chase *et al.*, 2015). After the mid-Miocene Climatic Optimum and inception of winter rainfall climate in the southwest, several cycles of climatic oscillations have been recorded, from warmer, wetter climates during interglacial periods to cooler, drier climates during glacial periods (Tyson, 1991; Demenocal, 1995, 2004; Zachos *et al.*, 2001; Hansen *et al.*, 2008)

The present paper examines the effects of these geomorphological and climatic changes on the genus, *Epirinus* Dejean,1833, which is endemic to southern Africa. *Epirinus* is monophyletic as inferred from both morphological (Medina & Scholtz, 2005) and molecular data (Mlambo, Sole, & Scholtz, 2011; Daniel *et al.*, 2020a). Biogeographically, it is distributed within eSwatini (formerly Swaziland) and from northeast to southwest regions of South Africa with the highest species diversity in

the southeast (Daniel *et al.*, 2020a). Recently, an outlier occurrence of a single widespread species has been documented from Namibia (Deschodt, Davis, & Daniel, 2019; Fig. 1). *Epirinus* species occur predominantly in both lowland forest and open vegetation of the southwest lowlands and northeast uplands. Fewer species occur in upland forests or open vegetation of southwest uplands. However, historical events that have affected the tempo and mode of diversification of *Epirinus* have not been investigated. In view of its endemism, the genus is a particularly interesting model system to understand the evolutionary effects behind shifts in habitat within southern Africa and link these events to key aspects of its biology. Thus, this paper aims to determine the range and vegetation type occupied by the ancestor of *Epirinus* and how late Cenozoic climatic fluctuations and resulting vegetation changes would have affected speciation and extinction of *Epirinus* species. Furthermore, using ecological niche modelling we predict the possible influences of global warming on the genus.

MATERIAL AND METHODS

PHYLOGENETIC ANALYSIS

SAMPLING, AMPLIFICATION, PROCESSING OF SEQUENCES AND ALIGNMENT

The dataset includes 17 of the 32 known species of *Epirinus.* Of these, two (*Epirinus asper* and *E. mucrodentatus*) were newly sequenced, while the rest were sourced from Genbank (Mlambo *et al.*, 2011). Based on the recent Sisyphini phylogeny (Daniel *et al.*, 2020a), two species of the sister genus, *Sisyphus*, are included as outgroup taxa, *Sisyphus* (*Neosisyphus*) *macrorubrus* and *S.* (*Parasisyphus*) *muricatus* (for Genbank accession numbers, see Daniel *et al.,* 2020a). For the new sequences, we amplified four gene regions. These comprised two nuclear genes: CAD (carbamoyl-phosphate synthetase 2, aspartate transcarbamylase, and dihydroorotase) and 28S rDNA (28S rDNA domain 2), and two mitochondrial genes: 16S (16S rDNA) and COI (cytochrome c oxidase subunit I). For details of the primers used for PCR amplification as well as extraction, amplification and sequencing protocols see Daniel *et al.* (2020a). Sequences were viewed, assembled and edited in CLC Main workbench version 7.0 (developed by CLC Bio, http://www.clcbio.com).

They were aligned using MAFFT web interface (Katoh & Toh, 2008) at the default settings.

PHYLOGENETIC ANALYSES

Phylogenetic analyses were performed under both Maximum likelihood (ML) and Bayesian inference (BI) frameworks. The combined datasets for four gene regions comprised a total of 2264 bp (base pairs); COI = 703 bp; CAD = 765 bp; 28S (D2) ≈ 496 bp; 16S ≈ 300 bp. We partitioned our data sets using PartitionFinder software v 2.1 (Lanfear *et al.*, 2016). The appropriate model selection and partitioning (Table 1) was determined under the corrected Akaike Information Criterion (AIC). We define the codon positions (1^{st}, 2^{nd}, 3^{rd}) for the two protein-coding genes (COI and CAD). The non-coding genes (16S and 28S) are regarded as a single data block.

MAXIMUM LIKELIHOOD

Maximum likelihood analyses were performed on each gene individually, and on the total concatenated data set. All ML analyses were implemented in RAxML v 8.2.4 (Stamatakis, 2014). Since RAxML allows only a single model of rate heterogeneity in partition analyses, we implemented the General Time Reversible model of nucleotide substitution under the GAMMA model of rate heterogeneity (Stamatakis, 2014). Nodal support confidence of the majority-rule consensus tree topology was estimated from 1000, non-parametric, bootstrap replicates of likelihood (Felsenstein, 1981, 1985).

BAYESIAN INFERENCE

Individual gene and concatenated phylogenies were also estimated through Bayesian Inference in MrBayes v 3.2.6 (Ronquist & Huelsenbeck, 2003). PartitionFinder was used to find the best-fit partitioning schemes and models of evolution. Bayesian analyses consisted of 10 million iterations with a random starting tree, and two simultaneous runs with four Markov chains sampled every 200th iteration. The first 25% of sampled trees were discarded as burn-in to ensure that the analysis had converged properly, which was determined by TRACER v 1.6

(Rambaut *et al.*, 2014). The credibility of clade support was provided by posterior probability estimation, summarised by majority-rule consensus in MrBayes.

DIVERSIFICATION TIME ESTIMATION

The node ages for the major lineage-splitting events within *Epirinus* were estimated using BEAST v 2.4.5 (Bouckaert *et al.*, 2014). As there is no fossil record for the genus *Epirinus*, we constrained the age of the root using the oldest reliably validated fossil in the subfamily of Scarabaeinae as suggested by Daniel *et al*. (2020a, b). The estimated age of this fossil (*Lobateuchus parisii*) is 53 Ma (Tarasov *et al.*, 2016). Furthermore, the age estimate of the outgroup (Sisyphini) by Gunter *et al*. (2016) is broadly in line with the fossil calibration, which supports using this fossil as a maximum age to constrain our analysis, with a standard deviation of 8.25 Myr, the other priors were at default settings. We used a Bayesian strict molecular clock analysis under the birth death process, with a normal distribution model approach. The combined data set was partitioned using PartitionFinder (see Table 1). We implemented a separate GTR + G substitution for each partition, following the BEAST v 2.4.5 default settings (Bouckaert *et al.*, 2014). Two independent MCMC analyses were run for 10 million iterations with parameters sampled at each 200th iteration. The first 25% of trees sampled in each run were discarded as burn-in. We used LogCombiner (BEAST 2 package) to combine the log and tree output files from the two independent runs. TRACER v 1.6 assessed the convergence between runs. We used TreeAnnotator (BEAST 2 package) to generate the consensus tree and determine the mean ages under 95% highest posterior density (HPD). The tree topologies were visualised in FigTree v 1.4.3 (Rambaut, 2009), including those from BI and ML analyses.

BIOGEOGRAPHICAL ANALYSIS

We conducted ancestral range reconstruction for *Epirinus* in southern Africa using the R package 'BioGeoBEARS' (Matzke, 2013). Three models of biogeographic inferences were considered: Dispersal-Extinction-Cladogenesis (DEC) (Ree & Smith, 2008), a maximum likelihood version of dispersal-vicariance analysis (DIVALIKE) (Ronquist, 1997), and a likelihood interpretation of Bayesian biogeographic inference

(BAYAREALIKE) (Landis *et al.*, 2013). For each model, we repeated the analysis with a founder-event speciation parameter, +J (Matzke, 2014). To determine the best model of biogeographic inference we assessed the fit of six model combinations (Table 2) based on the AIC scores and Akaike weights. For all models, the analyses were conducted using nine South African biomes (Mucina, Geldenhuys, & Rutherford, 2006, Fig. 1A): (A) Nama Karoo; (B) Kalahari Savanna; (C) Grassland; (D) East Savanna; (E) Albany Thicket; (F) Fynbos / Renosterveld; (G) Succulent Karoo; (H) Desert; (I) Forest. The distribution data for *Epirinus* species was sourced from taxonomic revisions (Scholtz & Howden, 1987; Medina & Scholtz, 2005; Deschodt *et al.*, 2019) and an atlas for southern African dung beetles (Davis, Deschodt & Scholtz, in press, see Tables S1–S2). The same procedure was applied to infer the type of vegetation likely occupied by the ancestor of *Epirinus*, i.e. forest / shaded versus open habitats.

DIVERSIFICATION ANALYSES

The diversification analyses were performed on an ultrametric tree topology with branch lengths scaled to time. A plot of lineage through time (LTT) (Nee *et al.*, 1995) was calculated using the R (R Core Team, 2019) package 'APE' (Paradis, Claude, & Strimmer, 2004). We also used the compound Poisson process on mass extinction times (CoMET) as implemented in the R (R Core Team, 2019) package 'TESS' (Höhna, May, & Moore, 2016; May, Höhna, & Moore, 2016) to estimate speciation and extinction rates through time. The compound Poisson process allows us to detect shifts in speciation or extinction rates that may be correlated with geoclimatic changes in southern Africa since the late Cenozoic. We ran a constrained MCMC analysis where the mean speciation rate (λ), mean extinction rate (μ) and their standard deviations are set to zero, which generated the posterior distributions of these hyper-priors (May *et al.*, 2016). These distributions were then used as hyper-priors in a full Bayesian analysis. The prior on the number of mass extinction events was set to 1.0. The reversible jump MCMC chains were run for 1 million generations with a burn-in of 25% and sampling thinning interval of 100.

ECOLOGICAL NICHE MODELLING

Based on the current distributions of *Epirinus* species in southern Africa sourced from the southern Africa dung beetle database (http://vmus.adu.org.za/, see Table S3); ecological niche modelling was performed under the maximum entropy (MaxEnt) algorithm (Phillips, Anderson, & Schapire, 2006; Phillips & Dudík, 2008) using past, current and future bioclimatic factors to predict the potential suitability of areas during Last Glacial Maximum, LGM (~22 000 years ago), mid-Holocene (~6 000 years ago), present-day and future (representative concentration pathways, RCP=8.5 in 2070).

As suggested by Daniel *et al.* (2020b) we chose our variables based on the knowledge of seasonal activity including feeding and nesting biology of the dung beetle subfamily, Scarabaeinae (Daniel *et al.*, 2020b). Therefore, six bioclimatic predictor variables were sourced from the WorldClim database version 2.0 (http://www.worldclim.org/; Hijmans *et al.*, 2005). The bioclimatic predictor variables were: BIO1 – annual mean temperature; BIO5 – maximum temperature of the warmest month; BIO6 – minimum temperature of the coldest month; BIO12 –annual precipitation; BIO13 – precipitation of the wettest month; BIO14 – precipitation of the driest month. We used the *Biogeo* v.1 R v 3.5.0 (Core Team, 2019) package (Robertson, Visser, & Hui, 2016) for cleaning and improving the quality of data for species occurrence including wrong environment and duplicate records. Furthermore, we used the “cor” function in R v 3.5.0 (Core Team, 2019) to minimise the autocorrelation among the selected bioclimatic variables (Merow, Smith, & Silander Jr, 2013). The environmental predictors were projected onto a background of Köppen-Geiger climate zones (Kottek *et al.*, 2006; Rubel & Kottek, 2010) with special adaptation to the following extent: 0, 50; -40, 0, under the spatial resolution of 2.5 arc -min (≈5 km^2 polygons) (F. Rubel, personal communication to GMD).

We fitted 10 replicate models in MaxEnt to run with a random seed. Occurrence data were divided into 75% training and 25% test points against a background of 10000 pseudo absence points. All other parameters were left at default settings. Although the area under the curve (AUC) is widely used as a metric of model performance, there is considerable debate about its suitability (Lobo, Jiménez-Valverde, & Real, 2008; Escobar *et al.*, 2018) even though, recent studies are still using this metric of

model performance (Shcheglovitova & Anderson, 2013; Boria & Blois, 2018; Galante *et al.*, 2018). Therefore, our modelling performance was evaluated using the average values of the AUC of the receiver operating characteristic curve (ROC) (Elith *et al.*, 2011).

RESULTS

PHYLOGENETIC RELATIONSHIPS AND DIVERGENCE-TIME ESTIMATION

The monophyly of the genus *Epirinus* is strongly supported by a Bayesian posterior probability of 1.0 and Maximum Likelihood bootstrap value of 100% (Fig. 2). The phylogenetic tree comprises two main clades; I (three spp.) and II (14 spp.), which is sub-divided into subclades; A (five spp.) and B (nine spp.). The genus *Epirinus* split from *Sisyphus* in the Oligocene, followed by diversification in the Miocene, respectively, clade I (17.3 Myr; 95% HPD interval: 23.0 to 15.0 Myr); clade IIA (15.11 Myr; 95% HPD interval: 17.0 to 13.0 Myr) and clade IIB (16.42 Myr; 95% HPD interval: 19.0 to 12.0 Myr) (Fig. 2).

ANCESTRAL RANGE ESTIMATION

The BioGeoBEARS model DEC+J and DEC show the best AIC scores for estimation of ancestral range for *Epirinus* (Tables 2–3, respectively). The most recent common ancestor most likely occupied a shaded vegetation type similar to that in the current Forest biome (Figs 3–4). Although there is a strong preference for shaded vegetation in the early diversification of *Epirinus,* independent shifts to open vegetation have been recovered (Fig. 4). Thus, several lineages of the genus have colonised various less-shaded, more open biomes throughout southern Africa probably from the Miocene onwards. Clade I is represented by three species with open vegetation or forest descendants. Clade IIA is represented by five species with forest descendants. Clade IIB is represented by nine species with primarily open vegetation descendants (Fig. 4).

The group comprising three species (clade I) includes a Miocene split between species that currently have lower scarp forest (*E. davisi*) or highland grassland affiliations. The grassland taxa have separated recently (Plio-Pleistocene) along the east escarpment into an extreme northeast species (*E. mucrodentatus*) and another

extending from highland grassland to the lowland forests of the Eastern Cape (*E. relictus*). The clade comprising 14 species shows an old Miocene separation into two clades IIA and IIB comprising five and nine species, respectively. Diversification of the five species commences in the Miocene and they currently show affiliations with forest patches on either side of the boundary (*E. minimus*) between the summer (*E. aquilus*, *E. convexus*, *E. sebastiani*) and bimodal rainfall regions (*E. silvestris*) on the south / southeast coast and coastal scarp. Diversification of the nine species also commences in the Miocene and they currently show affiliations with more open vegetation both to the southwest and northeast. *E. aeneus* shows a southwest distribution pattern. Species pairs *E. comosus* / *E. pygidialus* and *E. scrobiculatus* / *E. obtusus* show southwest or east / northeast patterns. Similarly, in the remaining species grouping, *E. flagellatus* shows a southwest pattern, *E. sulcipennis* a southeast coastal scarp pattern, *E. validus* an Eastern Cape to northeast pattern and *E. asper* an extreme northeast pattern. This represents similar patterns evolved over different time scales.

PATTERNS OF DIVERSIFICATION

Our LTT plot suggests that diversification of *Epirinus* lineages was intense from 17 Myr onward, flattening off somewhat at the beginning of Pliocene, followed by intense accumulation of lineages in the Plio-Pleistocene (Fig. 5A). The CoMET analysis shows low and relatively constant extinction rates up to the late Miocene but, at the end of the Miocene to the Plio-Pleistocene, the extinction rates somewhat increased. The speciation rate was constantly higher during the earlier period of diversification but declined in the mid-Miocene (Fig. 5B–D).

ECOLOGICAL NICHE MODELLING

Cross-validation of the climate envelope model showed a high mean fit with AUC>0.9, indicating good performance of the model (Table S4). During the LGM, high-suitability areas were larger than at present and were centred in the southwest, southeast coast and highveld grassland. During the mid-Holocene, the predicted higher suitability areas were relatively similar to the present-day and smaller than at the LGM. Future (2070) predictions add only two additional suitable spots in the

Nama-Karoo whereas highveld grassland regions will be transformed into a high suitability area. Otherwise, predicted high suitability areas are relatively similar to the present-day (Fig. 6).

DATA AVAILABILITY

The data that support the findings of this study are available in the Supporting Information section (Tables S1-S4). Sequence data are openly available at GenBank.

DISCUSSION

PHYLOGENETIC ANALYSIS

The monophyly of the genus *Epirinus* has been supported by Medina & Scholtz (2005), Mlambo *et al.* (2011), Daniel *et al.* (2020a) as well as the present study. Although sequences of a further two species (*E. mucrodentatus* and *E. asper*) are included in this new study, the species relationships are similar to Daniel *et al.* (2020a) and Mlambo *et al*. (2011), but the tree topology, nodal support values and branch-lengths diverge from those shown by Mlambo *et al.* (2011). . The differences could be because the data were not partitioned in the study of Mlambo *et al.* (2011) unlike in the present study and that of Daniel *et al*. (2020a) who applied the algorithmically optimised scheme selected under the Akaike information criterion (AIC). It should be noted that data set partitioning schemes in molecular systematics often affect tree topology and may, consequently, generate errors in phylogenetic inference (Brown & Lemmon, 2007; see also Kainer & Lanfear, 2015; Lemmon & Moriarty, 2004).

The late Oligocene split between *Epirinus* and *Sisyphus* is congruent within that proposed for “Sisyphini” by Gunter *et al.* (2016) using different schemes of calibrations as well as Epirinini + Sisyphini divergence from Daniel *et al.* (2020a) through secondary calibration under Yule clock model. The latter study corroborates with the current findings, supporting that the genus *Epirinus* diversified during the early Miocene. Furthermore, our age prediction is in line with previous estimations

using slow mutation rates (Sole & Scholtz, 2010; Mlambo *et al.*, 2011; Mlambo, Sole, & Scholtz, 2015).

SPECIATION PROCESSES IN *EPIRINUS*

Our results suggest that the most recent common ancestor of *Epirinus* was widely distributed in forest. However, using climatic biogeographical regionalisation and parsimony-based methods–DIVA, Daniel *et al.* (2020a) also suggest that *Epirinus* originated in the southern cool Winter / Bimodal Rainfall region to the south. It is therefore possible that the genus shows a cool forest origin with radiation into cool, more open vegetation following the inception of winter rainfall to the southwest and uplift of the highveld to the northeast.

There is a slight shift on the extinction rates and speciation for *Epirinus* shift in the mid-Miocene and Plio-Pleistocene (Fig. 5B–C), respectively. These periods coincide with three important phenomena, all of which are regarded to have a strong influence on the evolution of southern African biota (Cowling *et al.*, 2005). There was (a) a first uplift of the eastern region of southern Africa around 20 Myr followed by a second uplift during the Pliocene, 2–5 Myr in the southeast. The latter is thought to have isolated the interior plateau, contributing to aridification of the subcontinent (Partridge & Maud, 1987). After the mid-Miocene Climatic Optimum, (b) environmental conditions changed from moist and warmer to dry and cooler (Hansen *et al.*, 2008). During the transition between the Miocene and Pliocene, a winter rainfall regime was established in the southwestern region (Deacon, Jury, & Ellis, 1992) coupled with the intensification of semi-arid conditions in the western portion of southern Africa (Scott, Anderson, & Anderson, 1997). In the early to mid-Miocene (20–10 Myr), (c) grassland ecosystems widely dominated the region, replacing riparian and temperate forests (Coetzee & Rogers, 1982; Cerling *et al.*, 1997; Mucina *et al.*, 2006; Neumann & Bamford, 2015), probably due to decline in global temperatures and low levels of atmospheric CO_2 (Hansen *et al.*, 2008).

The most recent common ancestor of clade I is predicted to be a forest adapted species although of three extant descendants, one is found in forest and two in open

habitats (Fig. 4). The forest species, *E. davisi*, has a disjunct pattern of distribution associated with coastal and lower escarpment forest in the northeast region (Deschodt *et al.*, 2019). The ancestral area estimation suggests that the most recent common ancestor of a) *E. mucrodentatus* and b) *E. relictus*, was, itself, adapted to open habitats. It seems that the ancestor was split into geographically isolated populations in high altitudes under cooler conditions on the eastern escarpment and along the Drakensberg escarpment and southeast coast (Scholtz & Howden, 1987; Davis, Frolov, & Scholtz, 2008; Daniel *et al.*, 2020a), respectively. The age of these two daughter species matches the climatic cooling during the Plio-Pleistocene (Demenocal, 2004; Hansen *et al.*, 2008). Furthermore, the predicted age of these two species coincides with that of the second uplift in the southeast (Partridge & Maud, 1987). Hence, the regional impact of orogeny and climatic shifts might be responsible for the speciation of *E. mucrodentatus* and *E. relictus* during the Plio-Pleistocene (Figs 2–4).

The most recent common ancestor of clade IIA was probably centred in forest on the southeast coast (Figs 3–4). The diversification of the species in clade IIA seems to have started around 17–8 Myr, followed by climatic changes, from warmer, wetter to relatively cooler, drier conditions in the Plio-Pleistocene (Demenocal, 1995, 2004; Zachos *et al.*, 2001; Hansen *et al.*, 2008). This period coincides with the replacement of forest or closed habitats by grassland or savannah in southeastern Africa (Fernández & Vrba, 2006), due to the intensification of northern hemisphere glaciation (Demenocal, 1995, 2004; Zachos *et al.*, 2001; Zachos, Dickens, & Zeebe, 2008; Hansen *et al.*, 2008). Our ancestral range estimation (Figs 3–4) suggests that regional effects of these environmental and climatic changes are presumably responsible for fragmentation of the primaeval habitat of *Epirinus.* Shaded vegetation would have shrunk into the few southeastern, Afrotemperate, forest refugia in which they are found today. These extant species comprise an old and homogeneous lineage in respect to habitat. Therefore, the southeastern Cape is proposed as both a cradle and a refuge for *Epirinus*. Climatic refugia in southern Africa have been previously reported in mammals (Lawes *et al.*, 2007; Maswanganye *et al.*, 2017), reptiles (Tolley, Chase, & Forest, 2008; Barlow *et al.*, 2013; Nielsen *et al.*, 2018) and insects (Price, Barker, & Villet, 2007; Sole *et al.*, 2013; Switala, Sole, & Scholtz, 2014; Matenaar, Bröder, & Hochkirch, 2016; Strümpher *et al.*, 2016; Daniel *et al.*,

2020b; Hemp *et al.*, 2020), supporting the idea of climatically driven speciation of *Epirinus*.

The most recent common ancestor of clade IIB occupied open vegetation now found in a range of biomes from the southeast to southwest (Figs 3–4). Since the majority of the species in this clade are dated from late Miocene to Plio-Pleistocene, polar glaciation might have affected the radiation of this group. Polar glaciation in the Pliocene (Zachos *et al.*, 2001, 2008; Hansen *et al.*, 2008) coincides with the inception of winter rainfall seasonality in southern Africa (Deacon, 1983) and the upwelling of the cold Benguela current (Marlow *et al.*, 2000; Petrick *et al.*, 2015), which led to aridification in southwestern Africa (Diester-Haass, Meyers, & Bickert, 2004; Petrick *et al.*, 2015). All of these climatic trends intensified the conversion of closed habitats into open vegetation. In our study, it is evident that the disappearance of forest in association with climatic shifts after the mid-Miocene Climatic Optimum might have filtered out the more vulnerable species of *Epirinus.* This is supported by the slight increase of extinction rates in the last 8 Myr (Fig. 5C). Alternatively, some lineages of *Epirinus* were forced to colonise open habitats as shown in Fig. 3.

In addition, the late Cenozoic geomorphological changes in southern Africa could have affected the radiation of *Epirinus.* These events include the uplift of the Drakensberg escarpment and Highveld in the late Cenozoic (King, 1944; Partridge & Maud, 1987; Moore & Blenkinsop, 2006), which is linked to the deposition of deep sands in the Kalahari during the late Miocene (Haddon & McCarthy, 2005). Most importantly, this process changed the regional edaphic structure, and consequently, could have affected the evolution of local fossorial beetles (Davis *et al.*, 2016; Daniel *et al.*, 2020b) including *Epirinus*. Furthermore, higher temperatures in the Kalahari could be the primary barrier for a cool-adapted genus, since there are sand adapted *Epirinus* on the cool west coast of South Africa (Fig. 1A-B).

ECOLOGICAL NICHE MODELLING

As the predictions for the range-restricted area of the Cape Fold Mountains of South Africa (southeast and, to a lesser extent, the southwest) show a consistent climatic suitability from the past through to the future, ecological niche modelling identifies the region as a stable climatic refugium for *Epirinus* species through time (Fig. 6A-D). Additionally, unstable areas (upland areas in the interior of South Africa) suggest a recent habitat colonisation, possibly when forest habitats were converted into open vegetation.

The predicted differences in suitability between the future, present mid-Holocene and LGM suggest that *Epirinus* lineages have undergone and will undergo dramatic changes in population size and connectivity particularly in the southwest but also the northeast (Fig. 6A-D). However, caution should be taken as these simulations are based only on climatic data. Dung beetle distribution ranges are also influenced by favourable ecological conditions such as soil type, vegetation cover and specific dung type availability (Davis & Scholtz, 2020). Probably, the lack of these factors in our ecological niche modelling could explain why some localities of the current observed distribution of *Epirinus* species are not suitably represented in our prediction.

If current greenhouse gas emissions continue, the temperature will rise 3.5˚C by 2070 (Rintoul *et al.*, 2018). A few spots at high altitudes will become suitable for *Epirinus* in the central plateau of South Africa (Fig. 6A). This result is corroborated by a study of southern African birds, which predicted that warmer climates would drive many species to track suitable cooler conditions at higher altitude or more southerly latitudes (Coetzee *et al.*, 2009). Furthermore, a recent paper predicts that greatest effects of climate change in southern Africa will be on the west coast (Trisos, Merow, & Pigot, 2020). Our ecological niche modelling predicts colonisation of new localities and isolation in cooler “islands”, which might lead to speciation or maybe extinction in the long term. Our prediction is in line with previous studies that suggest an increase in temperature will, in all probability, promote massive extinction of taxa (Cahill *et al.*, 2013; Veron *et al.*, 2019; Wang *et al.*, 2020).

CONCLUDING REMARKS

Although our taxon sampling is incomplete, this study is a benchmark and model for evolution of southern African or beyond invertebrate fauna. The genus *Epirinus* is predicted to have a cool forest origin with radiation into three cool centres: (a) eastern escarpment forest and highland grassland; (b) southeastern Cape forest and (c) southwest to northeast in open vegetation at lower altitudes. Radiation of *Epirinus* centred in unshaded vegetation coincides with late Cenozoic climatic changes, including the inception of winter rainfall to the southwest and uplift of the highveld to the northeast. The droughts in southern Africa could have had the effect of an extensive shrinking of shaded vegetation, forcing an adaptation of forest inhabitants to upland grassland environments or driving some *Epirinus* species to extinction. The effect of climatic changes on the evolution of *Epirinus* is shown by slight decline in speciation rates during the mid-Miocene and an increase in extinction rates during the drier and cooler Plio-Pleistocene. These results support the climatically driven diversification of *Epirinus.*

In addition, we use ecological niche modelling across the past, present and future to assess how climatic change has and will affect distribution patterns of *Epirinus*. The southeast and, to a lesser extent, the west-coast regions are predicted as climatically stable areas for *Epirinus* species. The future projection suggests that *Epirinus* species will colonise new localities and that they will be isolated in upland “islands”, which might lead to speciation or extinction in the very long term.

ACKNOWLEDGEMENTS

CLS acknowledges the NRF for funding to generate the additional molecular data. GMD would like to express his gratitude to Professor Franz Rubel (University of Veterinary Medicine, Vienna) for providing the Köppen-Geiger climate zones of 2.5 arc min grid resolutions for southern Africa. Christian Deschodt is thanked for the image of habitus of *Epirinus* in Fig. 2. We thank Nicole Gunter, Bruno de Medeiros and two anonymous reviewers for their helpful comments. The authors declare there are no conflicts of interest.

REFERENCES

Barlow A, Baker K, Hendry CR, Peppin L, Phelps T, Tolley KA, Wüster CE & Wüster W. **2013**. Phylogeography of the widespread A frican puff adder (B itis arietans) reveals multiple P leistocene refugia in southern A frica. *Molecular Ecology* **22**: 1134–1157.

Boria RA & Blois JL. **2018**. The effect of large sample sizes on ecological niche models: analysis using a North American rodent, Peromyscus maniculatus. *Ecological Modelling* **386**: 83–88.

Bouckaert R, Heled J, Kühnert D, Vaughan T, Wu CH, Xie D, Suchard MA, Rambaut A & Drummond AJ. **2014**. BEAST 2: a software platform for Bayesian evolutionary analysis. *PLoS computational biology* **10**: e1003537.

Brown JM & Lemmon AR. **2007**. The importance of data partitioning and the utility of Bayes factors in Bayesian phylogenetics. *Systematic Biology* **56**: 643–655.

Cahill AE, Aiello-Lammens ME, Fisher-Reid MC, Hua X, Karanewsky CJ, Yeong Ryu H, Sbeglia GC, Spagnolo F, Waldron JB & Warsi O. **2013**. How does climate change cause extinction? *Proceedings of the Royal Society B: Biological Sciences* **280**: 20121890.

Cerling TE, Harris JM, MacFadden BJ, Leakey MG, Quade J, Eisenmann V & Ehleringer JR. **1997**. Global vegetation change through the Miocene/Pliocene boundary. *Nature* **389**: 153–158.

Chase BM, Lim S, Chevalier M, Boom A, Carr AS, Meadows ME & Reimer PJ. **2015**. Influence of tropical easterlies in southern Africa's winter rainfall zone during the Holocene. *Quaternary Science Reviews* **107**: 138–148.

Chase BM & Meadows ME. **2007**. Late Quaternary dynamics of southern Africa's winter rainfall zone. *Earth-Science Reviews* **84**: 103–138.

Coetzee BWT, Robertson MP, Erasmus BFN, Van Rensburg BJ & Thuiller W. **2009**. Ensemble models predict Important Bird Areas in southern Africa will become less effective for conserving endemic birds under climate change. *Global Ecology*

and Biogeography **18**: 701–710.

Coetzee JA & Rogers J. **1982**. Palynological and lithological evidence for the Miocene palaeoenvironment in the Saldanha region (South Africa). *Palaeogeography, Palaeoclimatology, Palaeoecology* **39**: 71–85.

Cowling RM, Procheş Ş, Vlok JHJ & Van Staden J. **2005**. On the origin of southern African subtropical thicket vegetation. *South African Journal of Botany* **71**: 1–23.

Daniel GM, Sole CL, Davis AL V, Strümpher WP & Scholtz CH. **2020a**. Systematics of the dung beetle tribe Sisyphini Mulsant (Scarabaeidae: Scarabaeinae) inferred from a molecular phylogeny and biogeography of southern African species. *Systematic Entomology* **45**: 73–84.

Daniel GM, Davis ALV, Sole CL & Scholtz CH. **2020b**. Evolutionary history and eco-climatic diversification in southern African dung beetle Sisyphus. *Journal of Biogeography* **47**: 2698–2713.

Dauteuil O, Bessin P & Guillocheau F. **2015**. Topographic growth around the Orange River valley, southern Africa: A Cenozoic record of crustal deformation and climatic change. *Geomorphology* **233**: 5–19.

Davis LVA. **1997**. Climatic and biogeographical associations of southern African dung beetles (Coleoptera: Scarabaeidae s. str.). *African Journal of Ecology* **35**: 10–38.

Davis AL V, Scholtz CH, Deschodt CM & Strümpher WP. **2016**. Edaphic and climatic history has driven current dung beetle species pool and assemblage structure across a transition zone in central South Africa. *Biological journal of the Linnean Society* **119**: 329–347.

Davis AL V, Frolov A V & Scholtz CH. **2008**. *The African dung beetle genera*. Protea Book House.

Davis AL V & Scholtz CH. **2001**. Historical vs. ecological factors influencing global patterns of scarabaeine dung beetle diversity. *Diversity and Distributions* **7**: 161–174.

Davis AL V & Scholtz CH. **2010**. Speciation and evolution of eco-climatic ranges in

the intertropical African dung beetle genus, Diastellopalpus van Lansberge. *Biological journal of the Linnean Society* **99**: 407–423.

Davis AL V & Scholtz CH. **2020**. Dung beetle conservation biogeography in southern Africa: current challenges and potential effects of climatic change. *Biodiversity and Conservation* **29**: 667–693.

Deacon HJ. **1983**. An introduction to the fynbos region, time scales and palaeoenvironments. In: Fynbos Palaeoecology: a Preliminary Synthesis (Eds H.J. Deacon, Q.B. Hendey and J.J. Lambrechts). *South African National Scientific Report*: 1–20.

Deacon HJ, Jury MR & Ellis F. **1992**. Selective regime and time. In 'The ecology of Fynbos: Nutrients, Fire and Diversity'.(Ed. RM Cowling) pp. 6–22.

Demenocal PB. **1995**. Plio-pleistocene African climate. *Science* **270**: 53–59.

Demenocal PB. **2004**. African climate change and faunal evolution during the Pliocene–Pleistocene. *Earth and Planetary Science Letters* **220**: 3–24.

Deschodt CM, Davis AL V & Daniel GM. **2019**. The endemic Southern African genus Epirinus Dejean, 1833 (Coleoptera: Scarabaeidae: Scarabaeinae) revisited: five new species and two new synonyms. *Zootaxa* **4603**: 327–340.

Diester-Haass L, Meyers PA & Bickert T. **2004**. Carbonate crash and biogenic bloom in the late Miocene: Evidence from ODP Sites 1085, 1086, and 1087 in the Cape Basin, southeast Atlantic Ocean. *Paleoceanography* **19**.

Elith J, Phillips SJ, Hastie T, Dudík M, Chee YE & Yates CJ. **2011**. A statistical explanation of MaxEnt for ecologists. *Diversity and distributions* **17**: 43–57.

Escobar LE, Qiao H, Cabello J & Peterson AT. **2018**. Ecological niche modeling re-examined: A case study with the Darwin's fox. *Ecology and evolution* **8**: 4757–4770.

Felsenstein J. **1981**. Evolutionary trees from DNA sequences: a maximum likelihood approach. *Journal of molecular evolution* **17**: 368–376.

Felsenstein J. **1985**. Confidence limits on phylogenies: an approach using the bootstrap. *Evolution* **39**: 783–791.

Fernández MH & Vrba ES. **2006**. Plio-Pleistocene climatic change in the Turkana Basin (East Africa): evidence from large mammal faunas. *Journal of Human Evolution* **50**: 595–626.

Galante PJ, Alade B, Muscarella R, Jansa SA, Goodman SM & Anderson RP. **2018**. The challenge of modeling niches and distributions for data-poor species: a comprehensive approach to model complexity. *Ecography* **41**: 726–736.

Gunter NL, Weir TA, Slipinksi A, Bocak L & Cameron SL. **2016**. If dung beetles (Scarabaeidae: Scarabaeinae) arose in association with dinosaurs, did they also suffer a mass co-extinction at the K-Pg boundary? *PloS one* **11**: e0153570.

Haddon IG & McCarthy TS. **2005**. The Mesozoic–Cenozoic interior sag basins of Central Africa: the late-cretaceous–Cenozoic Kalahari and Okavango basins. *Journal of African Earth Sciences* **43**: 316–333.

Halffter G & Matthews EG. **1966**. The natural history of dung beetles in the subfamily Scarabaeidae (Coleoptera, Scarabaeidae). *Folia Entomologica Mexicana* **12**: 1–312.

Hansen J, Sato M, Kharecha P, Beerling D, Berner R, Masson-Delmotte V, Pagani M, Raymo M, Royer DL & Zachos JC. **2008**. Target atmospheric CO2: Where should humanity aim? *arXiv preprint arXiv:0804.1126*.

Hemp C, Scherer C, Brandl R & Pinkert S. **2020**. The origin of the endemic African grasshopper family Lentulidae (Orthoptera: Acridoidea) and its climate-induced diversification. *Journal of Biogeography* **47**: 1805–1815.

Hijmans RJ, Cameron SE, Parra JL, Jones PG & Jarvis A. **2005**. Very high resolution interpolated climate surfaces for global land areas. *International Journal of Climatology: A Journal of the Royal Meteorological Society* **25**: 1965–1978.

Höhna S, May MR & Moore BR. **2016**. TESS: an R package for efficiently simulating phylogenetic trees and performing Bayesian inference of lineage diversification rates. *Bioinformatics* **32**: 789–791.

Kainer D & Lanfear R. **2015**. The effects of partitioning on phylogenetic inference. *Molecular biology and evolution* **32**: 1611–1627.

Katoh K & Toh H. **2008**. Recent developments in the MAFFT multiple sequence alignment program. *Briefings in bioinformatics* **9**: 286–298.

King LC. **1944**. Geomorphology of the Natal Drakensberg. *South African Journal of Geology* **47**: 255–282.

Kottek M, Grieser J, Beck C, Rudolf B & Rubel F. **2006**. World map of the Köppen-Geiger climate classification updated. *Meteorologische Zeitschrift* **15**: 259–263.

Landis MJ, Matzke NJ, Moore BR & Huelsenbeck JP. **2013**. Bayesian analysis of biogeography when the number of areas is large. *Systematic biology* **62**: 789–804.

Lanfear R, Frandsen PB, Wright AM, Senfeld T & Calcott B. **2016**. PartitionFinder 2: new methods for selecting partitioned models of evolution for molecular and morphological phylogenetic analyses. *Molecular biology and evolution* **34**: 772–773.

Lawes MJ, Eeley HAC, Findlay NJ & Forbes D. **2007**. Resilient forest faunal communities in South Africa: a legacy of palaeoclimatic change and extinction filtering? *Journal of Biogeography* **34**: 1246–1264.

Lemmon AR & Moriarty EC. **2004**. The importance of proper model assumption in Bayesian phylogenetics. *Systematic Biology* **53**: 265–277.

Lobo JM, Jiménez-Valverde A & Real R. **2008**. AUC: a misleading measure of the performance of predictive distribution models. *Global ecology and Biogeography* **17**: 145–151.

Marlow JR, Lange CB, Wefer G & Rosell-Melé A. **2000**. Upwelling intensification as part of the Pliocene-Pleistocene climate transition. *Science* **290**: 2288–2291.

Maswanganye KA, Cunningham MJ, Bennett NC, Chimimba CT & Bloomer P. **2017**. Life on the rocks: Multilocus phylogeography of rock hyrax (Procavia capensis) from southern Africa. *Molecular phylogenetics and evolution* **114**: 49–62.

Matenaar D, Bröder L & Hochkirch A. **2016**. A preliminary phylogeny of the South African Lentulidae. *Hereditas* **153**: 1.

Matzke NJ. **2013**. Probabilistic historical biogeography: new models for founder-event speciation, imperfect. *Issue: Frontiers of Biogeography, 5 (4)*.

Matzke NJ. **2014**. Model selection in historical biogeography reveals that founder-event speciation is a crucial process in island clades. *Systematic biology* **63**: 951–970.

May MR, Höhna S & Moore BR. **2016**. A Bayesian approach for detecting the impact of mass-extinction events on molecular phylogenies when rates of lineage diversification may vary. *Methods in Ecology and Evolution* **7**: 947–959.

Medina C & Scholtz C. **2005**. Systematics of the southern African genus Epirinus Reiche (Coleoptera: Scarabaeinae: Canthonini): descriptions of new species and phylogeny. *Insect Systematics & Evolution* **36**: 145–160.

Merow C, Smith MJ & Silander Jr JA. **2013**. A practical guide to MaxEnt for modeling species' distributions: what it does, and why inputs and settings matter. *Ecography* **36**: 1058–1069.

Mlambo S, Sole CL & Scholtz CH. **2011**. Phylogeny of the African ball-rolling dung beetle genus Epirinus Reiche (Coleoptera: Scarabaeidae: Scarabaeinae). *Invertebrate Systematics* **25**: 197–207.

Mlambo S, Sole CL & Scholtz CH. **2015**. A molecular phylogeny of the African Scarabaeinae (Coleoptera: Scarabaeidae).

Moore A & Blenkinsop T. **2006**. Scarp retreat versus pinned drainage divide in the formation of the Drakensberg escarpment, southern Africa. *South African Journal of Geology* **109**: 599–610.

Mucina L, Geldenhuys CJ & Rutherford MC. **2006**. Afrotemperate, subtropical and azonal forests. *The vegetation of South Africa, Lesotho and Swaziland. Strelitzia* **19**: 584–614.

Nee S, Holmes EC, Rambaut A & Harvey PH. **1995**. Inferring population history from molecular phylogenies. *Philosophical Transactions of the Royal Society of London. Series B: Biological Sciences* **349**: 25–31.

Neumann FH & Bamford MK. **2015**. Shaping of modern southern African biomes: Neogene vegetation and climate changes. *Transactions of the Royal Society of South Africa* **70**: 195–212.

Nielsen S V, Daniels SR, Conradie W, Heinicke MP & Noonan BP. **2018**. Multilocus phylogenetics in a widespread African anuran lineage (Brevicipitidae: Breviceps) reveals patterns of diversity reflecting geoclimatic change. *Journal of Biogeography* **45**: 2067–2079.

Paradis E, Claude J & Strimmer K. **2004**. APE: analyses of phylogenetics and evolution in R language. *Bioinformatics* **20**: 289–290.

Partridge TC & Maud RR. **1987**. Geomorphic evolution of southern Africa since the Mesozoic. *South African Journal of Geology* **90**: 179–208.

Paul JD, Roberts GG & White N. **2014**. The African landscape through space and time. *Tectonics* **33**: 898–935.

Petrick B, McClymont EL, Felder S, Rueda G, Leng MJ & Rosell-Melé A. **2015**. Late Pliocene upwelling in the Southern Benguela region. *Palaeogeography, palaeoclimatology, palaeoecology* **429**: 62–71.

Phillips SJ, Anderson RP & Schapire RE. **2006**. Maximum entropy modeling of species geographic distributions. *Ecological modelling* **190**: 231–259.

Phillips SJ & Dudík M. **2008**. Modeling of species distributions with Maxent: new extensions and a comprehensive evaluation. *Ecography* **31**: 161–175.

Price BW, Barker NP & Villet MH. **2007**. Patterns and processes underlying evolutionary significant units in the Platypleura stridula L. species complex (Hemiptera: Cicadidae) in the Cape Floristic Region, South Africa. *Molecular Ecology* **16**: 2574–2588.

Rambaut A. **2009**. FigTree.

Rambaut A, Suchard MA, Xie D & Drummond AJ. **2014**. Tracer 1.6. *URL: http://beast. bio. ed. ac. uk/tracer*.

Ree RH & Smith SA. **2008**. Maximum likelihood inference of geographic range evolution by dispersal, local extinction, and cladogenesis. *Systematic biology* **57**: 4–14.

Rintoul SR, Chown SL, DeConto RM, England MH, Fricker HA, Masson-Delmotte V, Naish TR, Siegert MJ & Xavier JC. **2018**. Choosing the future of

Antarctica. *Nature* **558**: 233–241.

Robertson MP, Visser V & Hui C. **2016**. Biogeo: an R package for assessing and improving data quality of occurrence record datasets. *Ecography* **39**: 394–401.

Ronquist F. **1997**. Dispersal-vicariance analysis: a new approach to the quantification of historical biogeography. *Systematic Biology* **46**: 195–203.

Ronquist F & Huelsenbeck JP. **2003**. MrBayes 3: Bayesian phylogenetic inference under mixed models. *Bioinformatics* **19**: 1572–1574.

Rubel F & Kottek M. **2010**. Observed and projected climate shifts 1901–2100 depicted by world maps of the Köppen-Geiger climate classification. *Meteorologische Zeitschrift* **19**: 135–141.

Rudge JF, Roberts GG, White NJ & Richardson CN. **2015**. Uplift histories of Africa and Australia from linear inverse modeling of drainage inventories. *Journal of Geophysical Research: Earth Surface* **120**: 894–914.

Scholtz CH & Howden HF. **1987**. A revision of the southern African genus Epirinus Reiche (Coleoptera: Scarabaeidae: Scarabaeinae). *Journal of the Entomological Society of southern Africa* **50**: 121–154.

Sciscio L, Tsikos H, Roberts DL, Scott L, van Breugel Y, Damste JSS, Schouten S & Grocke DR. **2016**. Miocene climate and vegetation changes in the Cape Peninsula, South Africa: Evidence from biogeochemistry and palynology. *Palaeogeography, Palaeoclimatology, Palaeoecology* **445**: 124–137.

Scott L, Anderson HM & Anderson JM. **1997**. Vegetation of Southern Africa. *Vegetation history*: 62–84.

Shcheglovitova M & Anderson RP. **2013**. Estimating optimal complexity for ecological niche models: a jackknife approach for species with small sample sizes. *Ecological Modelling* **269**: 9–17.

Sole CL, Scholtz CH, Ball JB & Mansell MW. **2013**. Phylogeny and biogeography of southern African spoon-winged lacewings (Neuroptera: Nemopteridae: Nemopterinae). *Molecular phylogenetics and evolution* **66**: 360–368.

Sole CL & Scholtz CH. **2010**. Did dung beetles arise in Africa? A phylogenetic

hypothesis based on five gene regions. *Molecular Phylogenetics and Evolution* **56**: 631–641.

Sole CL, Scholtz CH & Bastos ADS. **2005**. Phylogeography of the Namib Desert dung beetles Scarabaeus (Pachysoma) MacLeay (Coleoptera: Scarabaeidae). *Journal of Biogeography* **32**: 75–84.

Stamatakis A. **2014**. RAxML version 8: a tool for phylogenetic analysis and post-analysis of large phylogenies. *Bioinformatics* **30**: 1312–1313.

Strümpher WP, Sole CL, Villet MH & Scholtz CH. **2016**. Allopatric speciation in the flightless Phoberus capensis (Coleoptera: Trogidae) group, with description of two new species. *Insect Systematics & Evolution* **47**: 149–179.

Switala AK, Sole CL & Scholtz CH. **2014**. Phylogeny, historical biogeography and divergence time estimates of the genus Colophon Gray (Coleoptera: Lucanidae). *Invertebrate Systematics* **28**: 326–336.

Tarasov S, Vaz-de-Mello FZ, Krell FT & Dimitrov D. **2016**. A review and phylogeny of Scarabaeine dung beetle fossils (Coleoptera: Scarabaeidae: Scarabaeinae), with the description of two Canthochilum species from Dominican amber. *PeerJ* **4**: e1988.

Team RC. **2019**. R Project for Statistical Computing,(2019). *Available online: www. R-project. org/(accessed on 8 October 2014)*.

Tolley KA, Chase BM & Forest F. **2008**. Speciation and radiations track climate transitions since the Miocene Climatic Optimum: a case study of southern African chameleons. *Journal of Biogeography* **35**: 1402–1414.

Trisos CH, Merow C & Pigot AL. **2020**. The projected timing of abrupt ecological disruption from climate change. *Nature* **580**: 496–501.

Tyson PD. **1986**. *Climatic change and variability in southern Africa*. Oxford University Press, USA.

Tyson PD. **1991**. Climatic change in southern Africa: past and present conditions and possible future scenarios. *Climatic Change* **18**: 241–258.

Veron S, Mouchet M, Govaerts R, Haevermans T & Pellens R. **2019**. Vulnerability to climate change of islands worldwide and its impact on the tree of life. *Scientific*

Reports **9**: 14471.

Wang T, Zhu Q, Heller K, Zhou Z & Shi F. **2020**. Phylogenetic relationships and phylogeography of the genus Sinocyrtaspis Liu, 2000 (Orthoptera: Tettigoniidae: Meconematinae) reveal speciation processes related to climate change. *Systematic Entomology* **45**: 144–159.

Zachos J, Pagani M, Sloan L, Thomas E & Billups K. **2001**. Trends, rhythms, and aberrations in global climate 65 Ma to present. *science* **292**: 686–693.

Zachos JC, Dickens GR & Zeebe RE. **2008**. An early Cenozoic perspective on greenhouse warming and carbon-cycle dynamics. *Nature* **451**: 279–283.

Table 1. Data from PartitionFinder v 2.1: Subset partitions and best model used for phylogenetic inference analysis and estimate time divergence analyses.

Subset partition definitions	Partitions name	Best model
Subset 1=1-703	COI_pos1	GTR+G
Subset 2=2-703, 705-1468	CAD_pos2, COI_pos2	GTR+I+G
Subset 3= 3-703	COI_pos3	GTR+G
Subset 4=704-1468	CAD_pos1	GTR+I+G
Subset 5=706-1468	CAD_pos3	GTR+G
Subset6=1469-1768	16S	GTR+G
Subset7=1769-2264	28S	GTR+G

Table 2: Summary statistics of biogeographic model testing in 'BioGeoBEARS', in order to infer the most likely region occupied by the ancestors of *Epirinus*. The best fitting model is highlighted in bold. Values of parameters of dispersal (*d*), extinction (*e*), founder effect (*j*), likelihood scores (ln*L*), Akaike information criterion (AIC) are detailed.

Model	LnL	#Free parameters	d	e	j	AIC	AIC weight
DEC	-50,63	2	0,0086	1,00E-12	0	105,3	0,087
DEC+J	**-47,74**	**3**	**0,0069**	**1,00E-12**	**0,055**	**101,5**	**0,57**
DIVALIKE	-50,66	2	0,01	1,00E-12	0	105,3	0,084
DIVALIKE+J	-49,02	3	0,0082	1,00E-12	0,042	104	0,16
BAYAREALIKE	-66,13	2	0,01	0,01	0	136,3	1,60E-08
BAYAREALIKE+J	-49,53	3	0,0049	1,00E-07	0,13	105,1	0,096

Table 3: Summary statistics of biogeographic model testing in 'BioGeoBEARS', in order to infer the most likely ancestral vegetation type occupied by *Epirinus*. The best fitting model is highlighted in bold. Values of parameters of dispersal (*d*), extinction (*e*), founder effect (*j*), likelihood scores (ln*L*), Akaike information criterion (AIC) are detailed.

Model	LnL	#Free parameters	d	e	j	AIC	AIC weight
DEC	**-92,12**	**2**	**0,016**	**0,0095**	**0**	**188,2**	**0,51**
DEC+J	-91,52	3	0,013	1,00E-12	0,044	189	0,34
DIVALIKE	-93,72	2	0,016	0,0023	0	191,4	0,1
DIVALIKE+J	-93,38	3	0,015	1,00E-12	0,031	192,8	0,053
BAYAREALIKE	-99,12	2	0,01	0,01	0	202,2	0,0005
BAYAREALIKE+J	-98,79	3	0,01	0,01	0,0001	203,6	0,0002

Figures and captions

Figure 1A-B: Map showing biomes in southern Africa based on Mucina & Rutherford (2006) (A). The observed distribution of *Epirinus* species (B).

Figure 2. Phylogram of combined data set analysis (COI, 16S, CAD and 28S domain 2) for *Epirinus*. Maximum likelihood bootstrap (MLB), Bayesian posterior probabilities (PP) and relative estimated time of divergence indicated on clades of *Epirinus*. The blue bars in the main nodes represent the time intervals for the 95% probability of the actual age. The geological time scale represents millions of years ago (Myr).

Figure 3. Ancestral range reconstruction phylogram represents the biogeographical history of the genus *Epirinus* inferred under the DEC+J model in 'BioGeoBEARS'. The letters A-I represent biomes in southern Africa based on Mucina & Rutherford (2006): (A) Nama Karoo; (B) Kalahari Savannah; (C) Grassland; (D) East Savannah; (E) Albany Thicket; (F) Fynbos / Renosterveld; (G) Succulent Karoo; (H) Desert; (I) Forest.

Figure 4: Reconstruction of the ancestral habitat occupied by the ancestors of *Epirinus* inferred under the DEC+J model in 'BioGeoBEARS' (shaded *versus* open habitats). Pie charts show relative probabilities for ancestral range by colour at each node.

Figure 5A-C: *Epirinus* lineages through time (LTT) plots (A). Diversification analyses from TESS showing, extinction rates (B); speciation rates; (C) and net-diversification (D).

Figure 6A-D. Ecological niche modelling of the genus *Epirinus* in different geological periods using MaxEnt with bioclimatic factors. Future, year 2070 (RCP 8.5); (A) Present day (B); mid-Holocene (*c*. 6 ka) (C); Last Glacial Maximum (LGM, *c*. 22 ka) (D).The highest suitability area for species occurrence is represented by green colour.

SUPPORTING INFORMATION

Table S1: Southern African biomes and *Epirinus* association

Table S2: *Epirinus* vegetation types association, shaded vs unshaded

Table S3. Distribution data used for ecological niche modelling

Table S4: Niche ecological modelling statistics

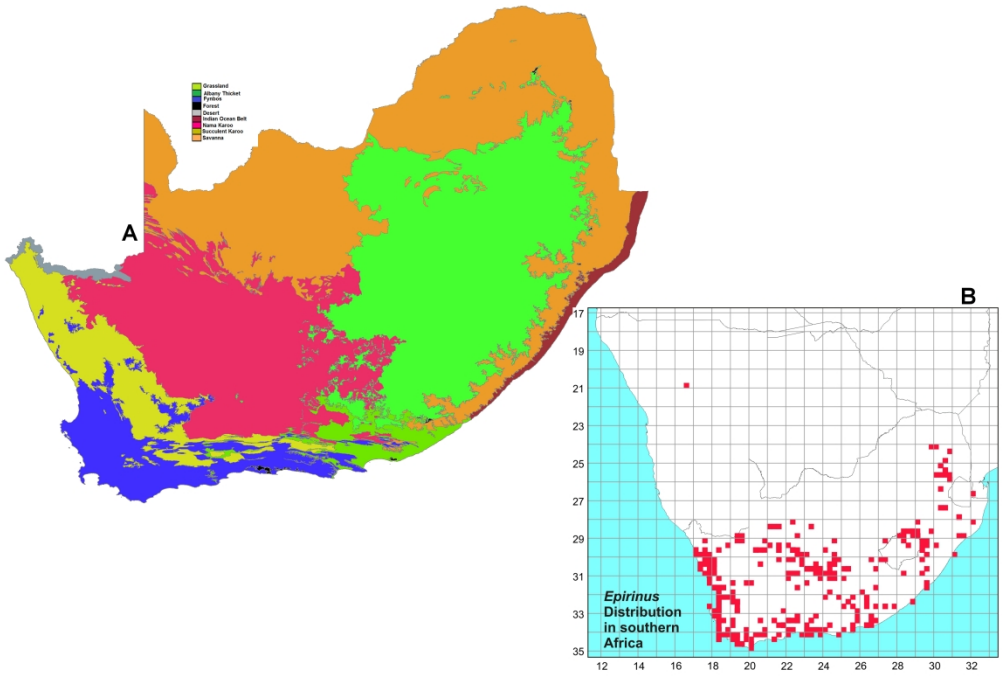

Figure 1A-B: Map showing biomes in southern Africa based on Mucina & Rutherford (2006) (A). The observed distribution of Epirinus species (B).

337x227mm (300 x 300 DPI)

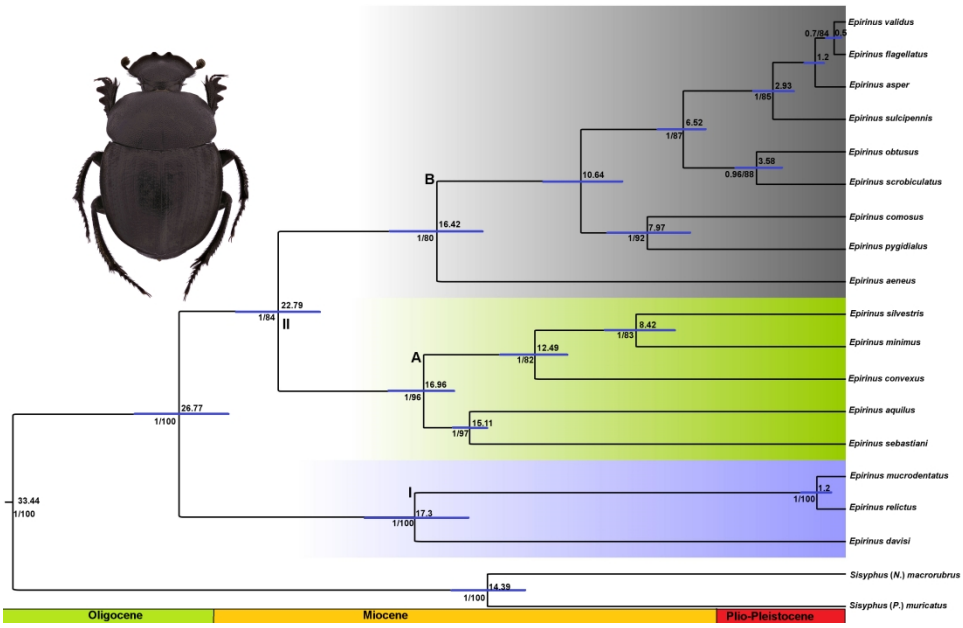

Figure 2. Phylogram of combined data set analysis (COI, 16S, CAD and 28S domain 2) for Epirinus. Maximum likelihood bootstrap (MLB), Bayesian posterior probabilities (PP) and relative estimated time of divergence indicated on clades of Epirinus. The blue bars in the main nodes represent the time intervals for the 95% probability of the actual age. The geological time scale represents millions of years ago (Myr).

27x17mm (3200 x 3200 DPI)

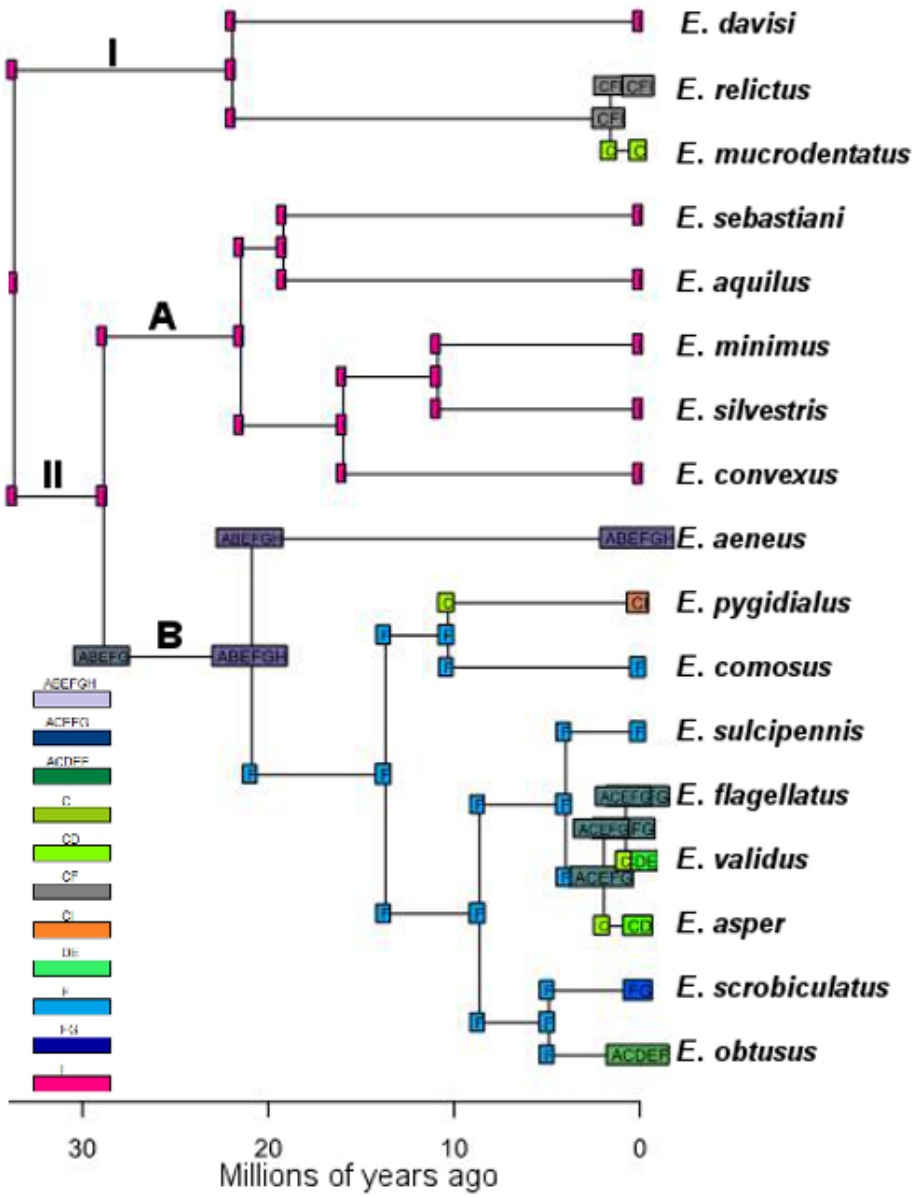

Figure 3. Ancestral range reconstruction phylogram represents the biogeographical history of the genus Epirinus inferred under the DEC+J model in 'BioGeoBEARS'. The letters A-I represent biomes in southern Africa based on Mucina & Rutherford (2006): (A) Nama Karoo; (B) Kalahari Savannah; (C) Grassland; (D) East Savannah; (E) Albany Thicket; (F) Fynbos / Renosterveld; (G) Succulent Karoo; (H) Desert; (I) Forest.

31x40mm (400 x 400 DPI)

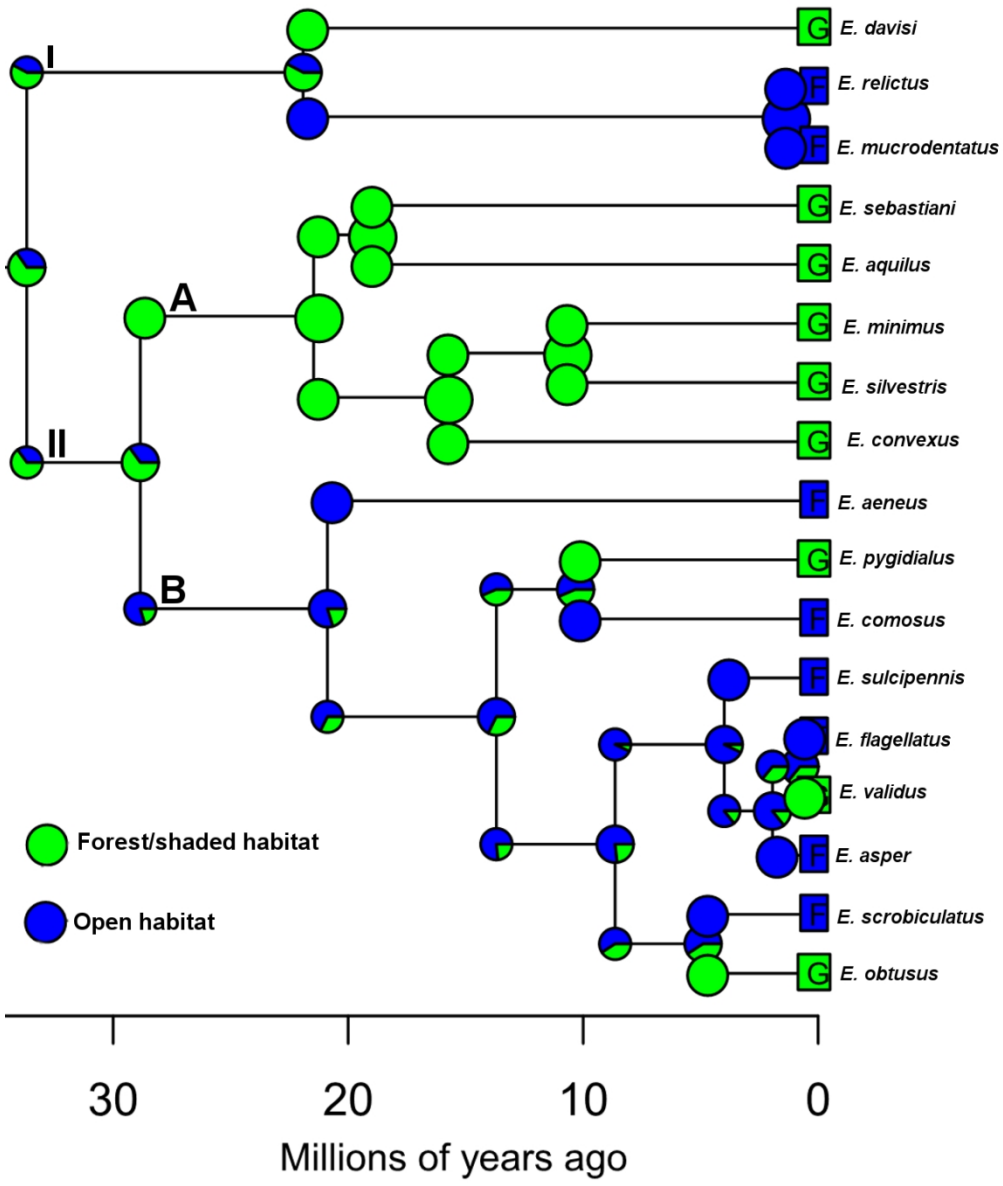

Figure 4: Reconstruction of the ancestral habitat occupied by the ancestors of Epirinus inferred under the DEC+J model in 'BioGeoBEARS' (shaded versus open habitats). Pie charts show relative probabilities for ancestral range by colour at each node.

81x96mm (401 x 401 DPI)

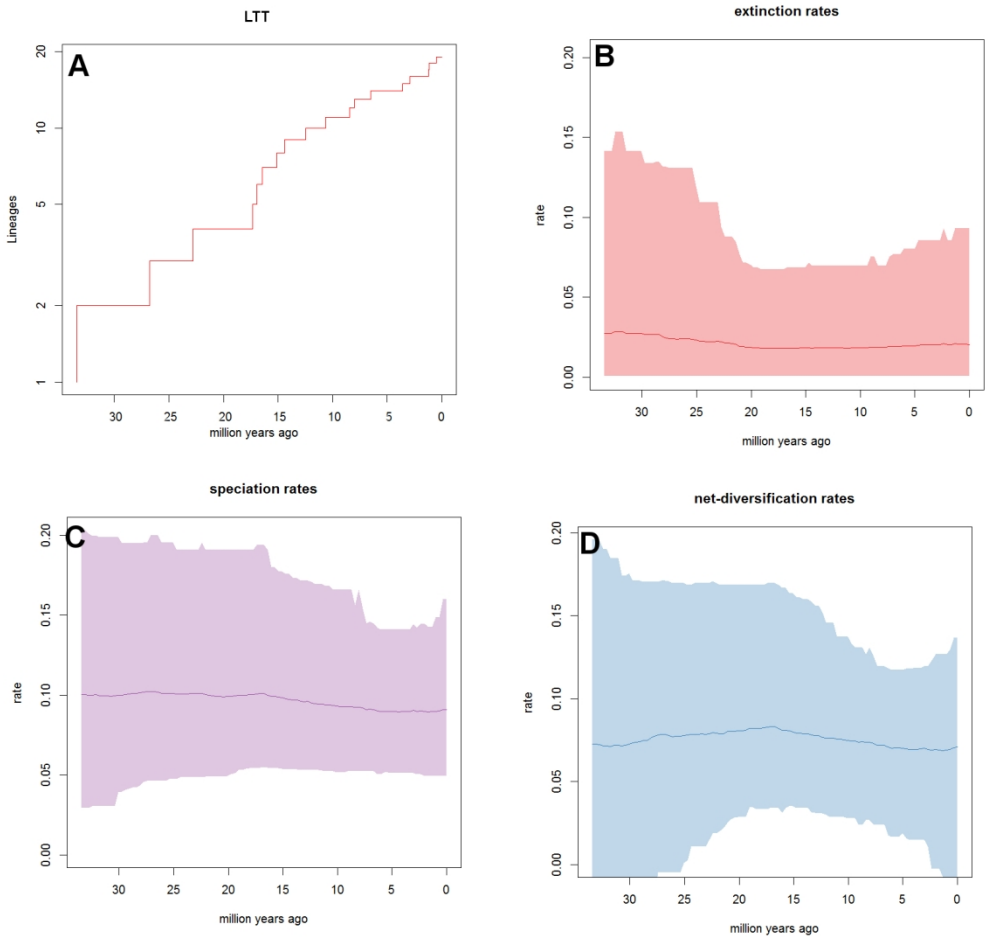

Figure 5A-C: Epirinus lineages through time (LTT) plots (A). Diversification analyses from TESS showing, extinction rates (B); speciation rates; (C) and net-diversification (D).

140x133mm (300 x 300 DPI)

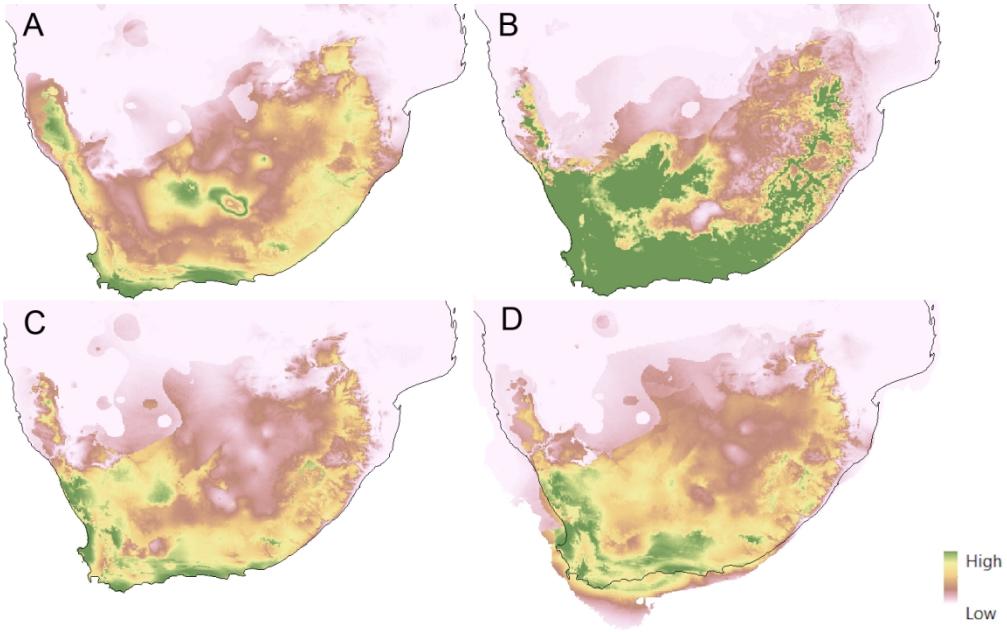

Figure 6A-D. Ecological niche modelling of the genus Epirinus in different geological periods using MaxEnt with bioclimatic factors. Future, year 2070 (RCP 8.5); (A) Present day (B); mid-Holocene (c. 6 ka) (C); Last Glacial Maximum (LGM, c. 22 ka) (D).The highest suitability area for species occurrence is represented by green colour.

415x261mm (96 x 96 DPI)

Table S1: Southern African biomes and *Epirinus* association

species	Nama Karoo	Kalahari Savanna	Grassland	East Savanna	Indian Ocean Coastal Belt	Albany Ticket	Fynbos	Succulent Karoo	Desert	Forest
E. davisi										x
E. relictus			x				x			
E. mucrodentatus			x							x
E. sebastiani										x
E. aquilus							x			x
E. minimus										x
E. silvestris										x
E. convexus					x					x
E. aeneus	*x*						x	x		
E. pygidialus			x				x			x
E. comosus							x			
E. sulcipennis							x			
E. flagellatus			x			x	x	x	x	
E. validus			x							
E. asper			x							
E. scrobiculatus							x	x		
E. obtusus			x			x				
NOT PRESENT IN OUR PHYLOGENY										
E. bentoi							x	x		
E. drakomontanus			x							
E. granulatus							x	x		
E. gratus		x	x							
E. hilaris						x	x			x
E. montanus							x			
E. pseudorugosus							x			
E. punctatus										x
E. rugosus							x			
E. striatus	*X*	x	x				x			
E. inparrugosus							x			
E. Jacobsae										x
E. muellerae			x							
E. pseudorelictus					x					
E. schoolmeestersi							x			

Table S2: *Epirinus* vegetation types association, shaded vs unshaded

species	Shaded habitat	Unshaded habitat
E. davisi	x	
E. relictus	x	x
E. mucrodentatus		x
E. sebastiani	x	
E. aquilus	x	
E. minimus	x	
E. silvestris	x	
E. convexus	x	
E. aeneus		x
E. pygidialus		x
E. comosus		x
E. sulcipennis		x
E. flagellatus		x
E. validus		x
E. asper		x
E. scrobiculatus		x
E. obtusus		x
Not present in our phylogeny		
E. bentoi		x
E. drakomontanus		x
E. granulatus		x
E. gratus		x
E. hilaris	x	x
E. montanus		x
E. pseudorugosus		x
E. punctatus	x	
E. rugosus		x
E. striatus		x
E. inparrugosus		x
E. Jacobsae	x	
E. muellerae		x
E. pseudorelictus		x
E. schoolmeestersi		x

Table S3. Distribution data used for ecological niche modelling

Species,"Longitude","Latitude"
Epirinus,22.61323,-29.58759
Epirinus,22.4046,-29.58627
Epirinus,22.34164,-29.60601
Epirinus,21.101639,-29.323917
Epirinus,23.003333,-29.778528
Epirinus,22.948611,-29.787917
Epirinus,22.79598,-30.37494
Epirinus,22.78834,-30.35298
Epirinus,22.751722,-29.965722
Epirinus,22.690833,-29.954333
Epirinus,22.83447,-30.33164
Epirinus,22.799806,-29.906083
Epirinus,22.813222,-29.917722
Epirinus,22.759944,-29.944472
Epirinus,22.59516667,-
28.91536111
Epirinus,22.663611,-29.972389
Epirinus,21.60303,-29.26742
Epirinus,21.63611,-29.28906
Epirinus,21.61614,-29.30289
Epirinus,20.87283333,-
29.62261111
Epirinus,23.54943,-30.88401
Epirinus,22.2327,-30.95319
Epirinus,22.24765,-30.9736
Epirinus,22.51742,-30.92419
Epirinus,22.49185,-30.93202
Epirinus,22.54619,-30.93494
Epirinus,22.39285,-30.07339
Epirinus,22.42647,-30.07464
Epirinus,22.42698,-30.00522
Epirinus,22.30626,-30.07439
Epirinus,22.27477,-30.05939
Epirinus,22.29097,-30.0345
Epirinus,22.98008,-29.85636
Epirinus,22.98548,-30.03299
Epirinus,22.95913,-30.04964
Epirinus,22.93532,-30.04598
Epirinus,22.90742,-30.03504
Epirinus,20.81274,-29.13895
Epirinus,20.76853,-29.13348
Epirinus,23.14322,-29.97907
Epirinus,20.45391,-29.55018
Epirinus,20.46513,-29.53105
Epirinus,20.50654,-29.55422
Epirinus,21.0832,-29.41027
Epirinus,21.09365,-29.43338

Epirinus,21.67735,-29.6118
Epirinus,21.65777,-29.59159
Epirinus,21.69467,-29.57419
Epirinus,22.144,-29.369306
Epirinus,22.3403,-30.11588
Epirinus,22.2173,-30.16422
Epirinus,20.217,-34.65
Epirinus,20.45,-34.05
Epirinus,18.25,-32.933
Epirinus,20.033,-34.533
Epirinus,18.35,-32.3
Epirinus,18.133,-33.167
Epirinus,19.033,-33.3
Epirinus,18.35,-33.067
Epirinus,19.45,-32.8167
Epirinus,20.2,-34.7
Epirinus,18.233,-31.533
Epirinus,17.833,-30.95
Epirinus,21.957,-32.824
Epirinus,18.317,-32.067
Epirinus,18.333,-31.993
Epirinus,18.421,-32.23
Epirinus,18.527,-32.249
Epirinus,18.429,-32.193
Epirinus,18.349,-32.191
Epirinus,18.733,-33.45
Epirinus,18.2,-31.633
Epirinus,18.432,-32.816
Epirinus,18.32,-32.785
Epirinus,18.283,-31.65
Epirinus,18.04,-32.86
Epirinus,18.416,-32.816
Epirinus,20.558,-30.32
Epirinus,18.067,-32.837
Epirinus,18.523,-31.721
Epirinus,18.353,-31.952
Epirinus,18.467,-34.267
Epirinus,18.433,-33.4
Epirinus,18.433,-33.417
Epirinus,18.4,-33.467
Epirinus,18.333,-33.467
Epirinus,23.609,-30.309
Epirinus,20.173,-31.297
Epirinus,22.441,-30.796
Epirinus,24.515,-29.206
Epirinus,17.933,-30.094
Epirinus,22.322,-28.194

Epirinus,19.333,-28.833
Epirinus,17.785,-29.844
Epirinus,23.68,-33.244
Epirinus,21.303,-28.431
Epirinus,21.701,-28.358
Epirinus,19.017,-31.383
Epirinus,23.031,-30.581
Epirinus,22.533,-33.167
Epirinus,17.99782,-30.97901
Epirinus,18.428611,-34.13556
Epirinus,18.3,-29.5167
Epirinus,21.533,-30.1167
Epirinus,18.9667,-29.2667
Epirinus,21.95,-33.733
Epirinus,17.9667,-32.7167
Epirinus,19.1667,-33.5
Epirinus,18.4,-32.283
Epirinus,18.4,-32.083
Epirinus,18.283,-32.65
Epirinus,18.5167,-34.0667
Epirinus,18.083,-30.4
Epirinus,19.383,-32.45
Epirinus,19.683,-29
Epirinus,19.6167,-28.8667
Epirinus,19.55,-34.633
Epirinus,20.05,-34.783
Epirinus,21.95,-33.7
Epirinus,21.7667,-33.7167
Epirinus,19.1667,-32.033
Epirinus,18.483,-32.2167
Epirinus,18.4667,-33.9667
Epirinus,20.155,-34.46
Epirinus,18.411,-33.422
Epirinus,19.12,-31.97167
Epirinus,21.233,-28.433
Epirinus,21.4167,-33.3667
Epirinus,17.7167,-30.783
Epirinus,29.2,-28.95
Epirinus,29.25,-29.033
Epirinus,30.033,-25.683
Epirinus,30.373,-25.615
Epirinus,30.717,-24.933
Epirinus,30.19501,-24.13272
Epirinus,29.5275,-29.200278
Epirinus,29.2167,-28.933
Epirinus,30.6667,-25.733
Epirinus,28.6025,-28.520833

Epirinus,30.459672,-25.097803
Epirinus,30.55,-25.25
Epirinus,30.8167,-25.783
Epirinus,29.233,-28.9667
Epirinus,29.433,-29.1167
Epirinus,29.782697,-28.553914
Epirinus,30.7667,-25.8667
Epirinus,29.983,-24
Epirinus,18.383,-33.933
Epirinus,19.95,-33.883
Epirinus,18.833,-34.117
Epirinus,18.45,-34.3
Epirinus,18.333,-34.083333
Epirinus,19.1667,-32.4
Epirinus,19.15,-32.383
Epirinus,19.433,-34.483
Epirinus,19.4167,-34.5167
Epirinus,18.85,-33.933
Epirinus,28.817,-32.25
Epirinus,29.533,-31.633
Epirinus,29.733333,-31.45
Epirinus,29.5,-31.55
Epirinus,26.4667,-32.683
Epirinus,31.466,-28.883
Epirinus,31.733,-28.833
Epirinus,32.067,-28.083
Epirinus,26.383,-33.717
Epirinus,24.8534,-34.19018
Epirinus,26.37136,-33.72194
Epirinus,31.417,-27.817
Epirinus,31.425,-27.835
Epirinus,21.707,-34.211
Epirinus,23.167,-33.833
Epirinus,19.217,-34.25
Epirinus,17.233,-29.6
Epirinus,19.323,-34.184
Epirinus,19.783,-31.467
Epirinus,18.267,-33.4
Epirinus,19.15,-32.483
Epirinus,18.913,-32.17
Epirinus,21.4,-34.267
Epirinus,18.102,-30.746
Epirinus,17.417,-30.5
Epirinus,18.45,-32.4
Epirinus,25,-33.948
Epirinus,22.967,-34.083
Epirinus,17.535,-29.744

Epirinus,17.492,-29.871
Epirinus,19.763,-34.389
Epirinus,19.183,-34.267
Epirinus,18.283,-31.067
Epirinus,19.6,-34.6
Epirinus,18.1,-30.983
Epirinus,19.75,-33.833
Epirinus,18.367,-32.583
Epirinus,17.933,-31.383
Epirinus,18.333,-32.6
Epirinus,20.724,-34.094
Epirinus,20.764,-34.098
Epirinus,19.316,-34.109
Epirinus,18.881,-33.755
Epirinus,22.6667,-33.417
Epirinus,19.167,-32.45
Epirinus,22.383,-33.883
Epirinus,20.85,-33.917
Epirinus,22.567,-33.4
Epirinus,18.017,-30.2
Epirinus,20.5,-33.267
Epirinus,19.1,-31.383
Epirinus,18.067,-30.45
Epirinus,26.85,-31.647
Epirinus,23.161,-33.577
Epirinus,27.45,-29.2
Epirinus,24.504,-30.43616
Epirinus,18.413611,-33.9622
Epirinus,19.2667,-32.5
Epirinus,28.513136,-29.351839
Epirinus,28.485872,-29.142972
Epirinus,23.483,-33.283
Epirinus,22.0464,-33.352
Epirinus,17.074167,-29.67778
Epirinus,17.223056,-29.84889
Epirinus,25.57,-33.918556
Epirinus,24.731667,-29.9922
Epirinus,22.6667,-33.4
Epirinus,19.2167,-32.433
Epirinus,24.363,-33.6
Epirinus,22.033,-33.333
Epirinus,19.2667,-32.4667
Epirinus,17.883,-30.733
Epirinus,17.45,-30.5667
Epirinus,17.586111,-29.240556
Epirinus,17.65,-29.9167
Epirinus,19.0667,-34.05

Epirinus,19.133,-33.5667
Epirinus,22.3167,-33.4167
Epirinus,22.3,-33.75
Epirinus,22.3167,-33.4
Epirinus,17.833,-31.1667
Epirinus,19.1167,-32.4667
Epirinus,17.8,-31.0667
Epirinus,17.1667,-29.783
Epirinus,25.754787,-33.483014
Epirinus,17.3167,-29.75
Epirinus,17.1667,-29.833
Epirinus,17.1167,-29.6667
Epirinus,17.1167,-29.7167
Epirinus,26.619722,-33.169167
Epirinus,28.2667,-28.833
Epirinus,21.633758,-33.728719
Epirinus,22.3667,-33.8667
Epirinus,18.45,-33.8
Epirinus,17.8667,-30.3667
Epirinus,26.769,-30.584
Epirinus,25.817,-32.75
Epirinus,25.45,-32.25
Epirinus,28.427,-30.979
Epirinus,29.41,-30.78
Epirinus,26.267,-32.017
Epirinus,26.195,-31.953
Epirinus,26.078,-31.925
Epirinus,24.467,-31.983
Epirinus,26.573,-30.074
Epirinus,29.347,-30.235
Epirinus,29.645767,-29.838467
Epirinus,25.1383,-32.5822
Epirinus,25.733,-32.233
Epirinus,26.533,-33.3167
Epirinus,25.588041,-32.721727
Epirinus,24.85,-32.15
Epirinus,23.667,-33.933
Epirinus,29.35515,-29.606917
Epirinus,29.303317,-29.594733
Epirinus,23.15,-33.933
Epirinus,30.2167,-29.3
Epirinus,17.417,-30.35
Epirinus,17.867,-31.117
Epirinus,18.517,-31.667
Epirinus,17.5,-30.383
Epirinus,18.05,-30.183
Epirinus,18.442778,-33.726111

Epirinus,18.333,-32.3667
Epirinus,18.2167,-30.95
Epirinus,18.096,-33.143
Epirinus,17.441351,-30.406473
Epirinus,23.167,-34.067
Epirinus,23.167,-33.95
Epirinus,23.2,-34.033
Epirinus,23.233,-34.083
Epirinus,23.883,-33.967
Epirinus,23.917,-34.017
Epirinus,23.2333,-34
Epirinus,23.273392,-34.033306
Epirinus,23.143186,-33.913825
Epirinus,23.033,-33.95
Epirinus,24.1667,-33.9667
Epirinus,26.083,-32.683
Epirinus,23.033,-34.033
Epirinus,26.717,-31.281
Epirinus,25.767,-31.583
Epirinus,28.917,-28.733
Epirinus,30.833,-24.25
Epirinus,30.433,-26.383
Epirinus,30.693,-27.487
Epirinus,29.28815,-29.586
Epirinus,29.174781,-28.249096
Epirinus,29.115321,-28.501024
Epirinus,29.5167,-29.433
Epirinus,30.271667,-27.296944
Epirinus,29.7,-30.6167
Epirinus,28.4667,-28.533
Epirinus,29.4667,-29.2667
Epirinus,28.1,-28.833
Epirinus,28.983,-28.683

Table S4: Niche ecological modelling statistics

Species/geological scale	Iterations	**Training AUC**	#Test samples	Test gain	Test AUC	AUC Standard Deviation	#Background points
Epirinus (average/2070)	500	**0,954**	99,3333	2,0082	0,9505	0,0049	10195,33
Epirinus (average/LGM)	500	**0,9593**	93	2,0762	0,9547	0,0048	10184,67
Epirinus (average/mid-Holocene)	500	**0,9611**	99,3333	2,1655	0,9575	0,0045	10194,67
Epirinus (average/present)	500	**0,9649**	104,3333	2,2803	0,9624	0,0041	10202